



Drawing lines while imagining circles: Neural basis of the bimanual coupling effect during motor execution and motor imagery



Francesca Garbarini ^{a,*}, Federico D'Agata ^{a,b,c}, Alessandro Piedimonte ^a, Katiuscia Sacco ^{a,b,d}, Marco Rabuffetti ^e, Fred Tam ^f, Franco Cauda ^{a,b,d}, Lorenzo Pia ^{a,d}, Giuliano Geminiani ^{a,b,d}, Sergio Duca ^b, Simon J. Graham ^{f,g}, Anna Berti ^{a,d}

^a Department of Psychology, University of Turin, Italy

^b CCS-fMRI, Koelliker Hospital and University of Turin, Italy

^c Department of Neuroscience, University of Turin, Italy

^d Neuroscience Institute of Turin (NIT), University of Turin, Italy

^e Biomedical Technology Department, Found. Don Carlo Gnocchi ONLUS, Milan, Italy

^f Physical Sciences, Sunnybrook Research Institute, Toronto, Canada

^g Department of Medical Biophysics, University of Toronto, Canada

ARTICLE INFO

Article history:

Accepted 25 October 2013

Available online 2 November 2013

Keywords:

Bimanual coupling effect

Motor execution

Motor imagery

Circles–Lines paradigm

Intention–programming system

fMRI

ABSTRACT

When people simultaneously draw lines with one hand and circles with the other hand, both trajectories tend to assume an oval shape, showing that hand motor programs interact (the so-called “bimanual coupling effect”). The aim of the present study was to investigate how motor parameters (drawing trajectories) and the related brain activity vary during bimanual movements both in real execution and in motor imagery tasks. In the ‘Real’ modality, subjects performed right hand movements (lines) and, simultaneously, Congruent (lines) or Non-congruent (circles) left hand movements. In the ‘Imagery’ modality, subjects performed only right hand movements (lines) and, simultaneously, imagined Congruent (lines) or Non-congruent (circles) left hand movements. Behavioral results showed a similar interference of both the real and the imagined circles on the actually executed lines, suggesting that the coupling effect also pertains to motor imagery. Neuroimaging results showed that a prefrontal–parietal network, mostly involving the pre-Supplementary Motor Area (pre-SMA) and the posterior parietal cortex (PPC), was significantly more active in Non-congruent than in Congruent conditions, irrespective of task (Real or Imagery). The data also confirmed specific roles of the right superior parietal lobe (SPL) in mediating spatial interference, and of the left PPC in motor imagery. Collectively, these findings suggest that real and imagined Non-congruent movements activate common circuits related to the intentional and predictive operation generating bimanual coupling, in which the pre-SMA and the PPC play a crucial role.

© 2013 Elsevier Inc. All rights reserved.

Introduction

If you perform simultaneous, Non-congruent movements with your hands, you will realize that each hand’s movement is affected by the movement of the other hand. Different kinds of modulation (both spatial and temporal) can be observed, depending on the action performed. These effects are collectively known as “bimanual coupling”. The present study focuses on the directional component of bimanual spatial coupling (Franz et al., 1991), involving functional magnetic resonance (fMRI) tasks in which Congruent (Lines–Lines) or Non-congruent (Circles–Lines) movements are executed by both hands (“Real” tasks), and tasks where the movements of one hand are performed while the movements (both Congruent and Non-congruent) of the other hand are only imagined (“Imagery” tasks). The study was designed to

investigate how motor parameters (drawing trajectories) and the related brain activity vary during bimanual Non-congruent movements, both in real execution and in motor imagery tasks.

In the classical Circles–Lines paradigm often used to reveal the reciprocal influence of hand actions in the spatial domain, subjects are asked to continuously draw straight lines with one hand and circles with the other. In this case, bimanual spatial coupling manifests as the tendency of both hand trajectories to assume an oval shape. In other words, lines tend toward circles and circles tend toward lines (Franz et al., 1991). The effect generalizes to bimanual tasks involving more discontinuous shapes, such as drawing squares combined with circles (Franz, 2003). It is important to note that, although the present study was only focused on directional features, spatial coupling effects may also pertain to amplitude parameters. In some previous studies, for example, amplitude parameters were manipulated by having subjects perform left and right limb movements with either the same or different amplitude specifications (for a review of spatial and other constraints, see Swinnen, 2002; Swinnen and Wenderoth, 2004; for experimental studies on

* Corresponding author at: Psychology Department, University of Turin, Via Po 14, 10123 Turin, Italy. Fax: +39 011 6703042.

E-mail addresses: francesca.garbarini@unito.it, fra.garbarini@gmail.com (F. Garbarini).

spatial interference with a directional and/or amplitude component, see Swinnen et al., 2001, 2002; Wenderoth et al., 2005a).

Other bimanual coupling effects have taken temporal parameters into account. Although a reliable temporal relationship exists between distance and time for simple unimanual reaching movements (different reaching distances imply different reaching durations), movement initiation and termination occur in a more coupled fashion during bimanual tasks with different target distances (Kelso et al., 1979; Pia et al., 2013). Similarly, healthy subjects who are asked to tap rhythms bimanually using non-harmonic relations are unable to produce two clearly distinct timing patterns without interference (Klapp, 1979; Peters, 1977). It is also well known that bimanual coordination in the mirror-symmetrical (in-phase) mode, in which homologous muscles are active simultaneously, is more stable than in the anti-parallel (out-of-phase) mode, in which homologous muscles are engaged in an alternating fashion (Swinnen et al., 1997). When subjects bimanually rotate disks with their index fingers in the out-of-phase mode, for example, increasing the movement frequency ultimately results in transition toward the in-phase mode, but the opposite transition does not occur (Kelso, 1984).

Many fMRI studies have investigated bimanual coordination, focusing on comparisons between unimanual and bimanual movements, and between in-phase and out-of-phase bimanual movements. The first comparison, between unimanual and bimanual movements, has been discussed primarily under two alternative hypotheses. One view argues that bimanual coordination is achieved by recruiting networks additional to those involved in unimanual hand movements (Debaere et al., 2004; Koeneke et al., 2004; Nair et al., 2003; Toyokura et al., 2002; Wenderoth et al., 2005b). The other view argues that a different temporal modulation of the same unimanual network is sufficient to sustain bimanual movement, without recruiting additional brain regions (e.g. Grefkes et al., 2008; Macaluso et al., 2007; Walsh et al., 2008). Very recently, it has been proposed that neural dynamics are dominated by temporal modulation of unimanual networks during execution of stable bimanual coordination patterns, with recruitment of additional areas during periods of instability or transition (Banerjee et al., 2012).

Converging neuroimaging data show that, in right-handed subjects, the (left) dominant hemisphere plays a principal role in performing bimanual symmetrical (in phase) movements, whereas the (right) non-dominant hemisphere has a key role during the execution of bimanual asymmetrical (out of phase) movements (Aramaki et al., 2006a; Maki et al., 2008; Meyer-Lindenberg et al., 2002; Sadato et al., 1997; Wenderoth et al., 2004). Within this right-brain network, the activity of certain brain areas has been described repeatedly. Increased activation during asymmetric movements has been observed in the dorsal premotor cortex (PMd) (Aramaki et al., 2006b; Sadato et al., 1997; Wenderoth et al., 2004); the cingulate motor area (CMA) (Ehrsson et al., 2002; Immisch et al., 2001); parietal areas (Diedrichsen et al., 2006; Ehrsson et al., 2002; Wenderoth et al., 2004, 2005a, 2005b); the cerebellum (Debaere et al., 2004; Nair et al., 2003); and in the Supplementary Motor Area (SMA) (Aramaki et al., 2006a; Debaere et al., 2004; Ehrsson et al., 2002; Immisch et al., 2001; Matsuda et al., 2009; Meyer-Lindenberg et al., 2002; Sadato et al., 1997).

The present study, incorporating both Real and Imagery tasks, was designed with two main goals: 1) to investigate the magnitude of spatial bimanual coupling during the Real and Imagery tasks; and 2) to evaluate and compare brain activity related to bimanual coupling for such task conditions. Previous studies have investigated the afferent versus efferent locus of bimanual coupling. These studies suggested that the interference effect cannot be modulated by manipulating afferent sources of information, and they concluded that spatial interference primarily emerges at the efferent level of movement planning and organization (Swinnen et al., 2003). Accordingly, in pathological conditions, spatial coupling effects should be observed even in the absence of actual movements of one hand. Garbarini et al. (2012) described bimanual coupling effects in left hemiplegic patients affected by anosognosia for

hemiplegia (denial of paralysis), who claimed to move their paralyzed hand when asked to draw lines with the right hand and circles with the left hand. Although no movement of the left hand occurred, lines drawn with the right hand showed clear “ovalization”. Using the same Circles–Lines paradigm, similar results were also found in amputees with illusory movements of the phantom limb (Franz and Ramchandran, 1998) and in brain-damaged patients affected by an atypical form of hemisomatoagnosia, who identified other people's limbs as belonging to themselves (Garbarini et al., 2013). In these lesional studies, the actual movement execution seemed unnecessary for bimanual coupling to occur: motor intention and programming was sufficient to trigger the interference effects.

This raises the question whether similar effects are present during a motor imagery task, in which normal subjects imagine that the left hand is drawing circles while the right hand is actually drawing lines. Many studies have shown that cerebral regions recruited during motor imagery and during motor execution overlap substantially (Ehrsson et al., 2003; Frak et al., 2001; Gerardin et al., 2000; Jeannerod and Frak, 1999; Parsons, 2001; Porro et al., 2000; Sacco et al., 2006), with brain activity during motor imagery associated more closely with that during the pre-executive (preparation) stage of real movement than that during the movement execution stage and analysis of sensory afferents (Hanakawa et al., 2008). Given the commonality of circuits between planned and imagined actions, it is reasonable to hypothesize that motor imagery triggers a similar motor intention-programming cascade of events as motor execution. If this is the case, then it is expected that, at the behavioral level, imagining drawing a circle with one hand will influence the trajectories of the other hand actively engaged in drawing lines. Importantly, although behavioral performance is difficult to assess in many imagery experiments, the tasks employed in the present study are designed to objectively and quantitatively reveal how imagery ability interacts with motor behavior, based on the amount of ovalization in line drawings.

Regarding the second goal of the present study, and based on the literature cited above, a similar brain activity is expected in both Real and Imagery tasks within the network related to the intention-programming system, mostly involving prefrontal–parietal circuits (e.g., Desmurget and Sirigu, 2009; Haggard, 2008). The use of both Real and Imagery tasks in the same study provides further information with respect to the existing pertinent functional neuroimaging literature involving actual movement execution. Specifically, the approach allows discrimination between two different components of bimanual coupling: one strictly related to actual execution of the Non-congruent movement, and the other related to selection and planning of the Non-congruent motor program. The first component is expected to be specific to the Real task; the second is expected to be common to both Real and Imagery tasks. Several lines of evidence suggest that two candidate brain regions will be crucially implicated in the latter prediction: medial wall motor areas, and parietal areas. For both areas, a role in bimanual movements has been previously described (e.g., Sadato et al., 1997; Wenderoth et al., 2004), as well as a functional distinction between regions subserving motor execution or motor intention and planning (e.g., Andersen and Buneo, 2002; Picard and Strick, 2001). In particular, based on the existing literature we predict that our experimental design will emphasize the functional role of the medial prefrontal and posterior parietal areas in the “abstract” selection of Non-congruent (CL) motor programs, irrespective of task (Real or Imagery).

Materials and methods

Subjects

Twelve healthy young subjects were recruited for the present study (mean age = 28.8, SD = 3.3). Two subjects were excluded from the analysis because of technical problems during data acquisition. All subjects had no history of psychiatric or neurological illness, and all were

2012, briefly summarized in the [Introduction](#)). Note that a “pure” Imagery task, in which subjects imagined bimanual movements (Congruent or Non-congruent), was not included because such a task would not allow a direct quantitative behavioral measurement to evaluate a potential coupling effect.

The timeline of each run comprised an initial 12-s rest followed by alternating 12-s experimental and rest blocks. A pseudorandom sequence of experimental blocks was presented to the subjects, comprising a total of 18 experimental blocks (6 repetitions for each of the 3 experimental conditions). During the rest blocks, a picture of two white hands (left and right) was presented on the monitor, instructing subjects to keep both hands still. During the experimental blocks, in the Real task, subjects performed self-paced hand movements based on the instructions (line or circle) appearing within the white hands. Subjects continuously drew vertical lines and/or circles, without interruption, for the entire duration of the block. Preliminary data showed that subjects were able to maintain a constant frequency between conditions automatically; consequently, subjects were directed to perform ecological, self-paced movements rather than imposing a fixed movement frequency. For the Imagery task, subjects imagined left hand movements when the picture of the left hand was colored blue. Subjects were instructed that during the Imagery task, they should “feel” themselves moving their hand (kinesthetic imagery), rather than picturing the movement in their “mind’s eye” (visuomotor imagery).

In a training period prior to fMRI, subjects viewed the task instructions (the pictures of the hands) on a computer monitor in the control room, and then performed the requested tasks by drawing on a sheet of paper. All subjects performed one practice block for each condition, including the rest condition. None reported problems learning the tasks.

Behavioral data collection and analysis

Dual panel fMRI-compatible tablet

The tablet was a modified version of the one used by [Tam et al. \(2011\)](#). Instead of one sensor panel and stylus, two separate panels and styli allowed the simultaneous collection of data from both hands (see [Fig. 2](#)). Each panel was connected to a distinct computer outside the scanner room for behavioral recording. To exclude the possibility that subjects would covertly generate small movements with their left hand during Imagery tasks, subjects were asked to hold the left stylus against the left tablet surface in these conditions. The behavioral recordings from all imagery blocks were visually inspected, and no movements were

recorded by the left tablet surface in most cases. Small oscillations due to trembling were observed in some cases, but none could be considered as real movements of interest.

Instrumented analysis of bimanual coupling during drawing

An Ovalization Index (OI) was defined to quantify the occurrence of lateral deviation when continuously drawing a straight vertical line. The strength of any bimanual coupling/interference effect was signaled by an increased OI value in the Non-congruent condition compared to the Congruent condition.

The raw measured trajectory of the stylus point (x = tablet lateral coordinates; y = tablet vertical coordinates) over successive up-and-down cycles was analyzed with the following steps to yield the OI value:

- 1) Removal of slow lateral drifts by subtracting an 8th-order polynomial fitting the time course of the lateral coordinate;
- 2) Reorientation of reference axes to identify “vertical” and “lateral” coordinates intrinsic to the recorded movements;
- 3) Temporal segmentation of the individual cycles by identification of the trajectory apical points (characterized by zero first derivative and negative second derivative);
- 4) Computation of the per-cycle ovalization according to the following formula:

$$OI_i = \frac{\text{stdev}(x_i)}{\text{stdev}(y_i)};$$

- 5) Computation of the OI value by determining the mean per-cycle ovalization of all recorded cycles per condition, for each subject.

The resulting OI has the following properties:

- a) A zero value for straight trajectories without any sign of ovalization, even if somewhat misaligned relative to the tablet’s vertical and horizontal axes;
- b) A value of 100 for circular trajectories;
- c) A value between 0 and 100 for oval trajectories with a longer vertical than lateral excursion;
- d) A value greater than 100 for oval trajectories with a longer lateral than vertical excursion (not expected).

Preprocessing of the recorded trajectories before calculation of the OI was implemented to exclude unwanted components that could otherwise add noise to the data and alter the OI value (steps 1 and 2 above).



Fig. 2. Dual panel fMRI-compatible tablet.

For example, some slow lateral drift and a slight difference between the vertical tablet axis and the vertical drawing direction are likely to arise during drawing performance, particularly without visual feedback.

Additionally, the average drawing frequency was computed for each block as the number of drawing cycles per second, or alternatively the inverse of the average cycle duration (in Hz).

Magnetic resonance imaging data acquisition

Data acquisition was performed using a 1.5-Tesla MR scanner (Intera, Philips Healthcare, Best, The Netherlands) with a Philips SENSE high-field, high resolution (MRIDC) 8-channel head coil optimized for functional imaging. T2*-weighted images were acquired with blood oxygenation level-dependent (BOLD) fMRI signal contrast using an echo planar imaging (EPI) sequence, with a repetition time (TR) of 3000 ms, an echo time (TE) of 60 ms, and a 90° flip angle. The acquisition matrix was 64 × 64; the field of view (FoV) was 256 mm². For each run, 148 volumes were acquired for a duration of 7 min 24 s per run. Each volume consisted of 25 axial slices, parallel to the anterior–posterior commissure (AC–PC) line and covered the whole brain; the slice thickness was 4 mm with a 0.5 mm gap. Two volumes were imaged (but not collected) at the beginning of each run to reach a steady-state magnetization, before subsequent acquisition of the experimental data.

In the same session, a set of three-dimensional high resolution T1-weighted structural images was acquired for each participant. This data set was acquired using a Fast Field Echo (FFE) sequence, with a repetition time (TR) of 2500 ms, minimum TE, and a 30° flip angle. The acquisition matrix was 256 × 256; the field of view (FoV) was 256 mm square. The data set consisted of 160 contiguous sagittal images covering the whole brain, with a voxel size of 1 mm × 1 mm × 1 mm.

fMRI data preprocessing and statistical analysis

The fMRI data were analyzed using BrainVoyager QX 2.3 (Brain Innovation, Maastricht, The Netherlands) with the following preprocessing steps: mean intensity adjustment, head motion correction, slice time correction, spatial smoothing (Gaussian full width at half maximum FWHM = 4 mm), linear trend removal, high pass filtering (cut-off >0.004 Hz) and temporal smoothing (FWHM = 2.8 s). After preprocessing, the fMRI data for each subject were co-registered to the associated 3D high resolution structural scan, which was transformed into Talairach space (Talairach and Tournoux, 1988). The preprocessed fMRI data were subsequently transformed into Talairach space using the anatomical–functional coregistration matrix and manually-determined Talairach reference points.

A single design matrix was specified for all subjects in each task condition, consisting of task-defined box-car time courses convolved with a predefined hemodynamic response function (HRF) (Boynton et al., 1996) to account for the hemodynamic delay. This design matrix was then entered into subject-level General Linear Model (GLM) analyses to yield beta parameter estimates for subsequent group statistics. At the group level, a 2 × 2 analysis of variance (ANOVA) was performed with Task (two levels, Real and Imagery) and Coupling (two levels, LL and CL) as within-subjects factors. The ANOVA was computed within a random effects GLM framework, with a regressor for subject, to yield brain activation maps. Tests for main effects and interaction effects were computed at a statistical threshold of $p < 0.005$ and then corrected for multiple comparisons ($p_{\text{cor}} < 0.05$) using cluster-size thresholding (Forman et al., 1995; Goebel et al., 2006). All bimanual versus unimanual contrasts (CL > L, L > CL for Real and Imagery; LL > L, L > LL for Real and Imagery) were analyzed using the same preprocessing, GLM, and statistical threshold procedures outlined above. See Supplementary Online Materials (SOM).

In addition, a conjunction test (Nichols et al., 2005) was performed to investigate voxels that were simultaneously activated by the coupling

effect (CL > LL) in both Real and Imagery conditions (threshold of $p < 0.01$, $p_{\text{cor}} < 0.05$ with cluster-size thresholding in both cases). See SOM. “Single-subject” region-of-interest (ROI) analyses were also undertaken, for pertinent ROIs in all subjects where activation results were observed for the Coupling factor in the group ANOVA. The ROI analyses focused on the contrast between CL and LL conditions in both Real and Imagery tasks, and on the conjunction of Real AND Imagery tasks. One caveat to these ROI analyses is that the group main effect of coupling used to define the ROIs is not orthogonal to the CL > LL contrast in either the Real or Imagery task, leading to a possible overestimation of the effects in single subjects. Consequently the ROI analyses should be considered supplementary support for the group analysis results, which are of primary interest in this work. See SOM.

A script (<http://precedings.nature.com/documents/6142/version/2>) was written in Matlab (The MathWorks, Inc., Natick, MA) to tabulate Talairach coordinates of local maxima of all activation maps and to determine the activated brain regions and Brodmann Areas (BA) according to the Analysis of Functional Neuroimages (AFNI, <http://afni.nimh.nih.gov>) atlas. The same script was used to compute the lateralization indices L% and R% for each cluster of brain activity, and for anatomical or BA subregions of clusters, according to the following formulae: $L = \frac{n_{\text{voxL}}}{n_{\text{voxL}} + n_{\text{voxR}}}$; $R = \frac{n_{\text{voxR}}}{n_{\text{voxL}} + n_{\text{voxR}}}$, where n_{voxL} is the number of active voxels in a cluster in the left cerebral hemisphere, n_{voxR} is the number of active voxels in the homologous region of the right hemisphere, and with L and R expressed as percentages. Activations were also classified using the method of Mayka et al. (2006) according to the related Human Motor Area Template (HMAT atlas, Tal Space AFNI Format, <http://irnlab.org>) that parcellated motor and somatosensory areas as: pre-Supplementary Motor Area (pre-SMA), SMA, PreMotor Cortex dorsal (PMCd), PMC ventral (PMCV), Primary Motor Cortex (M1), and Primary Somatosensory Cortex (S1). Cingulate areas immediately inferior to the pre-SMA and SMA were designated pre- and cingulate motor areas (pre-CMA and CMA), respectively.

Beta values were extracted from the brain activity determined by GLM analysis for both factors (Task and Coupling) to plot main and interaction effects. Beta values were also extracted from ROIs as determined by the Conjunction analysis (see SOM). To evaluate differences between brain regions while avoiding the “imager’s fallacy” (i.e. concluding meaningful differences between areas based on differences in the appearance of different parametric maps; Henson, 2005), paired t-tests were performed on the extracted beta values in CL and LL conditions. In particular, to investigate differences in medial wall motor areas, brain activity in front of and behind the anterior commissure was compared. Parietal activity in the right and left hemispheres was compared to investigate lateralization effects in the Real and Imagery tasks.

Results

Behavioral results

Based on the original investigation (Franz et al., 1991), the bimanual coupling effect for the right hand drawing lines in the Non-congruent condition (CL) should cause the Ovalization Index (OI) value to increase with respect to the baseline condition (L). No such increase in OI value is expected for the Congruent condition (LL). These expectations were confirmed for the Circles–Lines paradigm performed in the MR scanner, both in the Real and in the Imagery task. Illustrative examples of the right hand trajectories in different experimental conditions are shown in Fig. 3. Because frequency can influence trajectories in such tasks (Dounskaia et al., 2010), it is important to note that subjects automatically maintained a constant frequency between conditions, despite the self-paced task design. Two paired t-tests of drawing frequency mean values were performed for the contrast between LL and CL conditions in both Real (LL Mean ± SD: 1.32 ± 0.45 Hz; CL Mean ± SD: 1.31 ± 0.4 Hz)

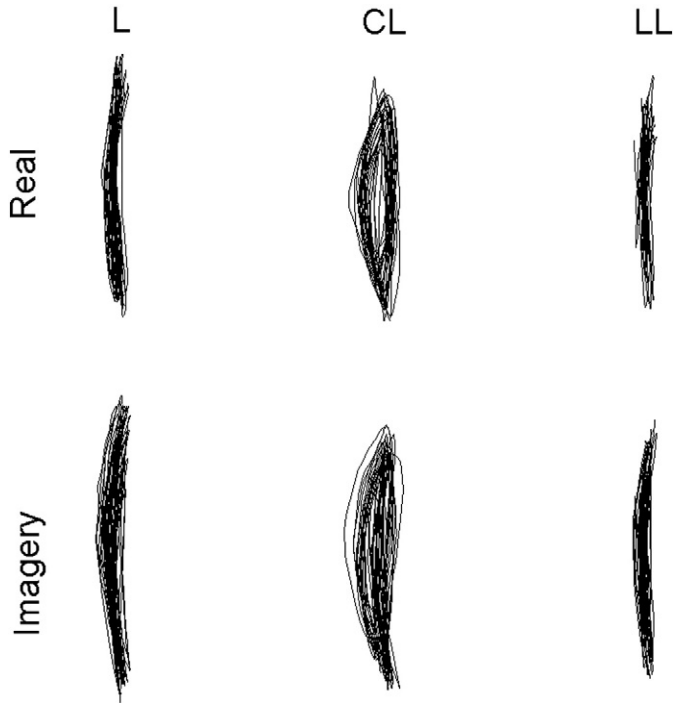


Fig. 3. Example of one subject's right hand trajectory for all experimental conditions (L; LL; CL) in both Real and Imagery tasks. Note the increased ovalization in the CL condition in both Real and Imagery tasks.

and Imagery (LL Mean \pm SD: 1.39 \pm 0.62 Hz; CL Mean \pm SD: 1.38 \pm 0.62 Hz) tasks. Overall, no significant difference was found for drawing frequency between these conditions (Real tasks: $p = 0.5$; Imagery tasks: $p = 0.6$). Because of this initial finding, drawing frequency was not included as a variable of interest in subsequent analyses.

A 2 \times 3 ANOVA of the OI mean value (averaging across both runs of each task, for all subjects) was computed with two within-subjects factors: Task (with two levels, Real and Imagery) and Condition (with three levels, L, LL and CL). The ANOVA showed a significant main effect of Condition ($F(2, 38) = 29.01$; $p = 0.000001$) and a significant Task \times Condition interaction ($F(2, 38) = 5.03$; $p = 0.01$). No main effect of Task was found ($F(1, 19) = 1.92$; $p = 0.2$). Duncan post hoc comparisons confirmed a significant difference between the CL and both L and LL conditions, in both the Real task ($p = 0.00003$ and $p = 0.00002$, respectively) and the Imagery task ($p = 0.0003$ and

$p = 0.0003$, respectively). The significant interaction was explained by the difference between Real CL and Imagery CL ($p = 0.0006$), suggesting that the increase in OI value, although present in both tasks, was significantly smaller in the Imagery task than in the Real task (Fig. 4).

These OI differences were consistently evident even at the single subject level. In 9 out of 10 subjects there was a significant (two-tailed t-test, $p < 0.05$ for each comparison) OI increase in the CL condition with respect to the L condition in both Real and Imagery tasks. On the contrary, none of the subjects showed a significant increase in the LL condition with respect to the L condition. Additionally, in 5 out of 10 subjects, the coupling effect above (CL > L) was significantly (two-tailed t-test, $p < 0.05$ for each comparison) smaller in the Imagery than in the Real task, as found in the group analysis. See Inline Supplementary Table S6.

Inline Supplementary Table S6 can be found online at <http://dx.doi.org/10.1016/j.neuroimage.2013.10.061>.

fMRI results

Main and interaction effects are reported below for the 2 \times 2 ANOVA that was performed to investigate the influence of Task (Real and Imagery) and Coupling (Congruent, LL; and Non-congruent, CL) on brain activity.

Task factor: Real versus Imagery

The main effect of the Task factor highlighted greater brain activity for the Real task (in which left hand movements were actually performed) compared to the Imagery task (in which left hand movements were only imagined). A right-lateralized sensorimotor network was implicated that included the right SMA proper (medial BA 6); the underlying CMA (BA 31); the right PMCV (lateral BA 6, BA 44); the right M1 (BA 4); bilateral S1 (BA 3 and BA 2); bilateral secondary somatosensory cortex (S2, BA 40); and the anterior vermis of cerebellum (vCRB). See Table 1 and Fig. 5a. Within this network, some areas, namely CMA, M1, S1 and vCRB, also participated in the main effect of the Coupling factor and the subsequent Interaction effect (see below). Greater activity was also observed for the Imagery task compared to the Real task in a left-lateralized network including the dorsolateral prefrontal cortex (DLPFC, BA 9); the dorsal PMC (PMCD, BA 6); the supramarginal gyrus (SMG, BA 40); and the left and right lateral posterior CRB. These activations did not survive multiple comparisons correction, however. Additionally, lateralization differed between the Real task (right lateralized) and the Imagery task (left lateralized) in the supplementary contrasts between bimanual conditions (CL and LL) and the unimanual right hand lines

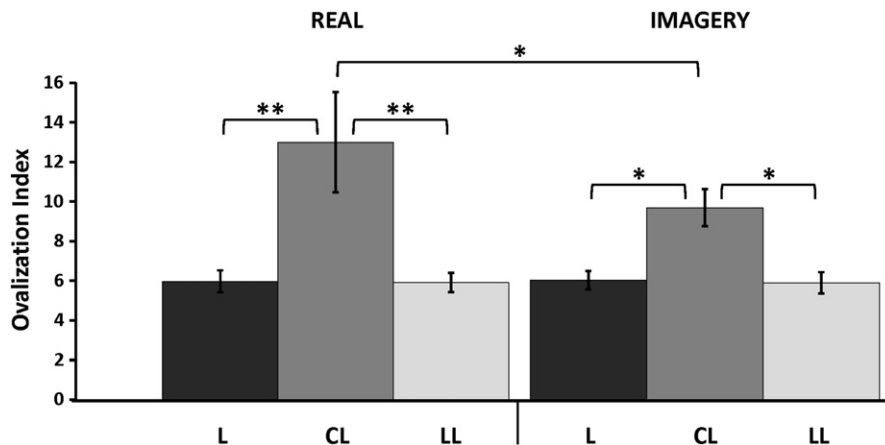


Fig. 4. Behavioral ANOVA results. Results of ANOVA with OI values for the right hand as the dependent variable and two between-subjects factors, Task (with two levels, Real and Imagery) and Condition (with three levels, L, LL and CL). Standard errors of the mean are shown. * $p < 0.0005$; ** $p < 0.00005$.

Table 1
Task factor.

| Cluster | Brain region | Ke | L/R% | x | Y | z | t | p |
|--------------------------|--|-----|-------|-----|-------|-------|------|----------|
| <i>Real > Imagery</i> | | | | | | | | |
| 1 | R Declive [vVI] Include: Culmen [vIV–V], Nodule [vX] | 260 | 71/29 | 2 | –62 | –18 | 8.89 | 0.000009 |
| 2 | R Postcentral Gyrus (BA 3)/S1 Include: Precentral Gyrus (BA 4)/M1, Inferior Parietal Lobule (BA 40)/S2 | 429 | 0/100 | 53 | –66.3 | –18.2 | 7.30 | 0.000046 |
| 3 | R Inferior Frontal Gyrus (BA 44)/PMv Include: Precentral Gyrus (BA 6)/PMv | 55 | 0/100 | 53 | 4 | 30 | 5.98 | 0.000206 |
| 4 | L Inferior Parietal Lobule (BA 40)/S2 Include: Postcentral Gyrus (BA 2) | 52 | 100/0 | –46 | –29 | 24 | 5.82 | 0.000253 |
| 5 | R Cingulate Gyrus (BA 31)/CMA Include: Medial Frontal Gyrus (BA 6)/SMA | 97 | 0/100 | 5 | –23 | 39 | 5.39 | 0.000439 |

Significantly activated clusters, $p < 0.05$, corrected for multiple comparisons using cluster-size thresholding (after $p < 0.005$ uncorrected). Ke = cluster extension in voxels ($3 \times 3 \times 3 \text{ mm}^3$). (BA) = Brodmann Area. L = Left. R = Right. x, y, z expressed in mm. v = Vermis, M1 = primary motor, S1 = primary sensory, S2 secondary sensory, PMv = PreMotor Ventral, CMA = Cingulate Motor Area, SMA = Supplementary Motor Area. Coordinates are in Talairach (big characters) and MNI (small characters) spaces. Brain regions were classified using AFNI (<http://afni.nimh.nih.gov>) and HMAT (<http://lrnlab.org>) atlases. Square brackets indicate Roman nomenclature of Schmahmann et al., 1999. Ratio between SMA and CMA = 42% and 58%.

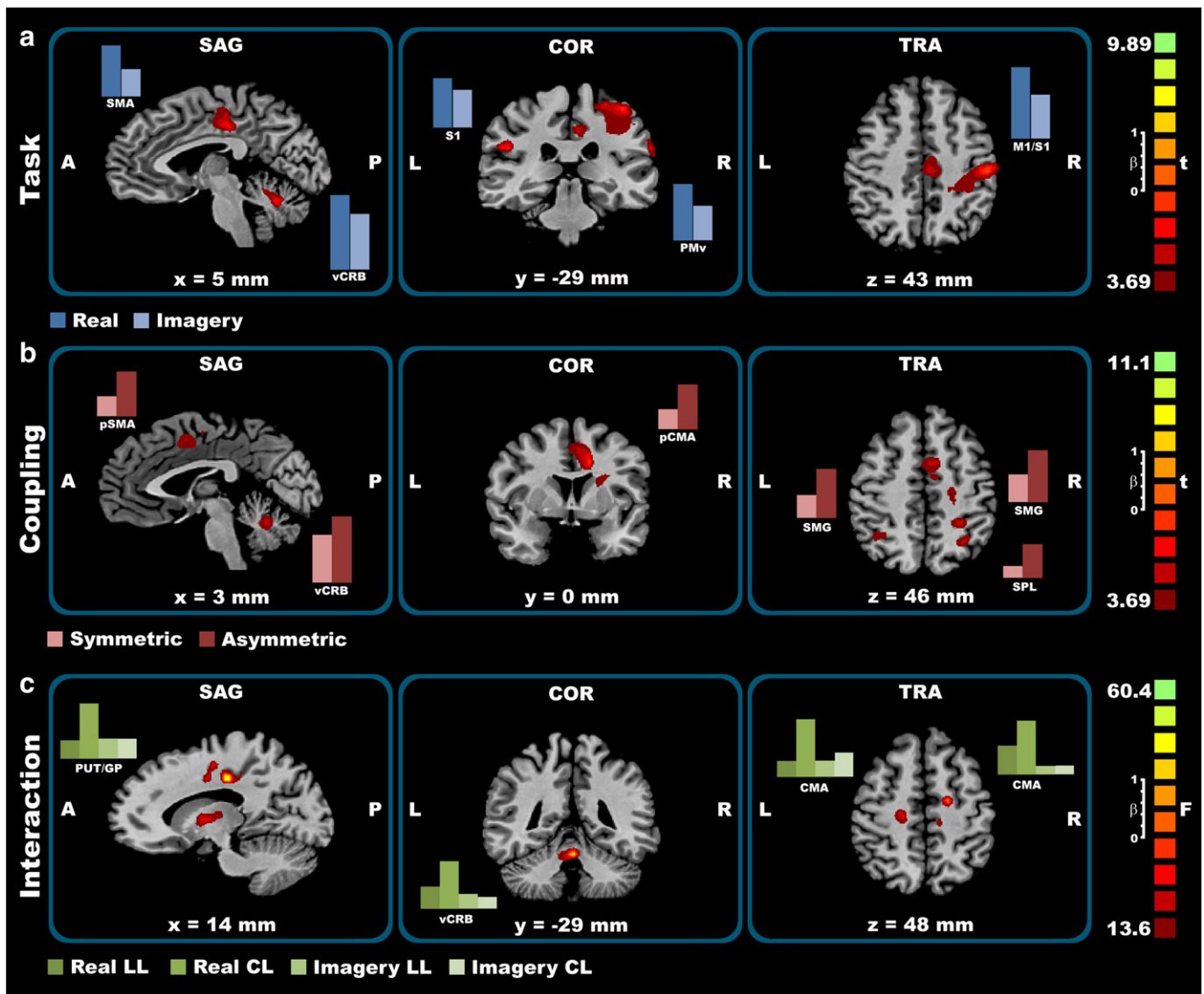


Fig. 5. fMRI ANOVA results. From top to bottom: a) Task effects; b) Coupling effects; c) Interaction effects. Significantly activated clusters, corrected for multiple comparisons at $p_{cor} < 0.05$ using cluster-size thresholding after $p < 0.005$ uncorrected). A = Anterior, P = Posterior. SAG = Sagittal, COR = coronal, TRA = Transverse. L = Left, R = Right. pSMA = preSMA, pCMA = preCMA. SMA = Supplementary Motor Area. M1 = primary motor area. S1 = primary motor area. CMA = Cingulate Motor Area. vCRB = vermis of cerebellum. SMG = Supramarginal Gyrus. SPL = Superior Parietal Lobule. PUT/GP = Putamen, Globus Pallidus. PMv = ventral Premotor Area. Statistical maps overlaid on a Talairach space template.

Table 2
Coupling factor.

| Cluster | Brain region | Ke | L/R% | x | Y | z | t | p |
|---------|---|-----|-------|--------------|--------------|--------------|-------|----------|
| 1 | R Cingulate Gyrus (BA 24)/pre-CMA; CMA Include: Medial Frontal Gyrus (BA 6)/pre-SMA; SMA | 187 | 1/99 | 14 16.7 | 7 13.0 | 39 37.5 | 10.08 | 0.000003 |
| 2 | R Inferior Parietal Lobule (BA 40) Include: Supramarginal Gyrus (BA 40) | 135 | 0/100 | 26 29.8 | −41 −38.3 | 36 39.0 | 7.22 | 0.000050 |
| 3 | L Declive [vVI] Include: Culmen [vIV–V], Nodule [vX] | 48 | 57/43 | −1 0.0 | −59 −63.2 | −18 −18.5 | 7.15 | 0.000054 |
| 4 | R Superior Parietal Lobule (BA 7) Include: Inferior Parietal Lobule (BA 40), Precuneus (BA 7) | 68 | 0/100 | 32 36.5 | −56 −53.0 | 48 53.8 | 5.96 | 0.000212 |
| 5 | L Inferior Parietal Lobule (BA 40) Include: Supramarginal Gyrus (BA 40) | 80 | 100/0 | −37 −38.3 | −47 −45.2 | 33 37.5 | 5.74 | 0.000280 |
| 6 | R Precentral Gyrus (BA 4)/M1 Include: Postcentral Gyrus (BA 3)/S1 | 73 | 0/100 | 23 26.7 | −20 −14.4 | 51 53.5 | 5.58 | 0.000343 |

Significantly activated clusters, $p < 0.05$, corrected for multiple comparisons using cluster-size thresholding (after $p < 0.005$ uncorrected). Ke = cluster extension in voxels ($3 \times 3 \times 3 \text{ mm}^3$). (BA) = Brodmann Area. L = Left. R = Right. x, y, z expressed in mm. v = Vermis, M1 = primary motor, S1 = primary sensory, CMA = Cingulate Motor Area, SMA = Supplementary Motor Area. Coordinates are in Talairach (big characters) and MNI (small characters) spaces. Brain regions were classified using AFNI (<http://afni.nimh.nih.gov>) and HMAT (<http://lrlab.org>) atlases. Square brackets indicate Roman nomenclature of Schmahmann et al., 1999.

Ratio between SMA and CMA = 36% and 64%

Ratio between pre-SMA and SMA = 64% and 36%

Ratio between pre-CMA and CMA = 64% and 36%.

condition (L). See SOM, Supplementary Fig. 1, Inline Supplementary Tables S1–S4.

Inline Supplementary Tables S1, S2, S3 and S4 can be found online at <http://dx.doi.org/10.1016/j.neuroimage.2013.10.061>.

Coupling factor: Non-congruent (CL) versus Congruent (LL) movement

The main effect of the Coupling factor revealed greater brain activity for the Non-congruent (CL) movements compared to the Congruent (LL) movements, irrespective of Real or Imagery task, in the form of a prefrontal–parietal network that included the right pre-SMA (mesial rostral BA 6); the underlying pre-CMA (BA 24); the bilateral posterior parietal cortex (PPC) particularly including the right superior parietal lobe (SPL, BA 7); the right precuneus (PrC); the bilateral inferior parietal lobe (IPL, BA 40); and the left and right supramarginal gyrus (SMG). These prefrontal and parietal areas were specific to the Coupling factor and were not found significant in the Task or Interaction effects. See Fig. 5b and Table 2. The activity of these coupling-specific areas was also evident in the conjunction analysis (Real AND Imagery) in the crucial contrast between bimanual Non-congruent CL and bimanual Congruent LL (Supplementary Fig. 2; Inline Supplementary Table S5) and in the contrast between bimanual Non-congruent CL and unimanual L in both the Real task (Supplementary Fig. 1b; Inline Supplementary Table S2) and the Imagery task (Supplementary Fig. 1d; Inline Supplementary Table S4). Activation of the right M1, the right S1, and the anterior vCRB, was also found for the main effect of Task (see above) and for the Task \times Coupling interaction (see below). No regions showed significantly greater activity in LL conditions than in CL conditions.

Inline Supplementary Table S5 can be found online at <http://dx.doi.org/10.1016/j.neuroimage.2013.10.061>.

Single-subject analysis showed, for most subjects, significant activity in the brain network for the coupling effect identified from the ANOVA group analysis. Moreover, between 8 and 9 out of 10 subjects (depending on the areas of the brain network) showed increased activity in the CL condition with respect to the LL condition, in both Real and Imagery tasks as shown in the conjunction analysis, reaching a significant level in 6 out of 10 subjects. See Inline Supplementary Table S7.

Inline Supplementary Table S7 can be found online at <http://dx.doi.org/10.1016/j.neuroimage.2013.10.061>.

Interaction Task \times Coupling: Real CL > LL versus Imagery CL > LL

The Task \times Coupling interaction revealed right-lateralized motor regions in which brain activity for the contrast between CL and LL was

always greater in the Real task than in the Imagery task: the bilateral CMA (BA 31); the bilateral PMCd (BA 6); the right M1 (BA 4); the right basal ganglia, including right lateral globus pallidum (GP) and right putamen (PUT); and the anterior vCRB. See Fig. 5c and Table 3.

For all analyses performed, plots of the lateralization (both in Gyrus and Brodmann areas) are shown in SOM (Supplementary Figs. 3–18).

Discussion

Using both Real and Imagery tasks, the present study was designed to discriminate between two different components of bimanual coupling: one strictly related to the execution of bimanual movement; and the other related to the abstract selection of (Non-congruent) motor programs, which was expected to be required for both motor execution and motor imagery. The behavioral results show that spatial coupling effects occur not only during actual execution of bimanual Non-congruent movements (the Real task), but also when the movements of one hand are only imagined (the Imagery task). The neuroimaging results first indicate that a right motor network is strongly associated with the actual execution of the left hand movements during a bimanual task. Second, and most importantly, they emphasize that a prefrontal–parietal network (mostly involving right pre-SMA/CMA and bilateral PPC) is responsible for the main effect of the Coupling factor, discriminating between Congruent (LL) and Non-congruent (CL) movements, both when Non-congruent movements are actually produced, and when they are only imagined.

From a behavioral point of view, although the coupling effect was present in both Real and Imagery tasks, the intensity was different, with stronger coupling occurring in the Real task than in the Imagery task (Fig. 4). In a previous study (Garbarini et al., 2012) a difference between motor execution and motor imagery was also found in a control group of elderly subjects. However, contrary to the results found in the young adults studied here, the coupling effect for the Imagery task was not statistically significant in the elderly group, although a trend was present. Motor imagery capacity can be impaired with age (Mulder et al., 2007; Personnier et al., 2008; Saimpont et al., 2009; Skoura et al., 2008) and different results for elderly (mean age 68.5, Garbarini et al., 2012) and young subjects (mean age: 28.8, the present study) are in keeping with this possibility.

In the fMRI results, a right motor network (including SMA, CMA, PMCV, M1, S1, S2, and vCRB) was found to be more active in the Real task than in the Imagery task (Fig. 5a). This network undoubtedly

Table 3
Interaction Task × Coupling.

| Cluster | Brain region | Ke | L/R% | x | Y | z | F | p |
|---------|---|----|-------|-------|-------|-------|------|----------|
| 1 | R Cerebellar Lingual [vI–II] | 44 | 58/42 | 2 | −44 | −18 | 59.4 | 0.000030 |
| | Include: Culmen [vIV–V] | | | 3.1 | −47.2 | −20.1 | | |
| 2 | R Cingulate Gyrus (BA 31)/CMA | 79 | 0/100 | 11 | −23 | 39 | 55.9 | 0.000038 |
| | Include: Precentral Gyrus (BA 6; 4)/PMd; M1 | | | 13.6 | −18.9 | 40.8 | | |
| 3 | R Lateral Globus Pallidus | 81 | 0/100 | 17 | −2 | 9 | 46.1 | 0.000080 |
| | Include: Putamen | | | 19.5 | 0.3 | 5.1 | | |
| 4 | L Cingulate Gyrus (BA 31)/CMA | 22 | 100/0 | −16 | −26 | 51 | 33.9 | 0.000253 |
| | Include: Precentral Gyrus (BA 6)/PMd | | | −15.4 | −21.0 | 54.9 | | |

Significantly activated clusters, $p < 0.05$, corrected for multiple comparisons using cluster-size thresholding (after $p < 0.005$ uncorrected). Ke = cluster extension in voxels ($3 \times 3 \times 3 \text{ mm}^3$). (BA) = Brodmann Area. L = Left. R = Right. x, y, z expressed in mm. v = Vermis, M1 = primary motor, PMd = PreMotor Dorsal, CMA = Cingulate Motor Area. Coordinates are in Talairach (big characters) and MNI (small characters) spaces. Brain regions were classified using AFNI (<http://afni.nimh.nih.gov>) and HMAT (<http://lrlab.org>) atlases. Square brackets indicate Roman nomenclature of Schmahmann et al., 1999. Ratio between SMA and CMA = 14% and 86%.

played a role in the actual movement execution of the left hand performing lines (in the LL condition) or circles (in the CL condition). More interestingly, however, some of these areas (CMA, M1, S1 and vCRB) were also active as part of the main effect of the Coupling factor (in $\text{CL} > \text{LL}$) and in the Task × Coupling interaction effect, where the difference in activity between the CL and LL conditions was greater in the Real task than in the Imagery task (Figs. 5b and c). In all three cases, these areas were mainly lateralized in the right hemisphere, confirming a right lateralization for the actual execution of bimanual Non-congruent movement (Aramaki et al., 2006a, 2006b; Maki et al., 2008; Meyer-Lindenberg et al., 2002; Sadato et al., 1997; Wenderoth et al., 2004). Other right hemisphere areas involved in motor execution, namely the PMCd and the basal ganglia (the globus pallidus, GP; and the putamen, PUT), participated in the interaction effect.

Importantly, as predicted, the results also showed that some pre-frontal–parietal areas (the right pre-SMA/pre-CMA and the bilateral PPC) showed neither a Task effect nor an Interaction effect, but were active for the main effect of Coupling, discriminating between Congruent (LL) and Non-congruent (CL) movements, irrespective of task (Real or Imagery) (Fig. 5b). To exclude the possibility that the main effect of Coupling was driven almost entirely by the Real CL condition, even given the lack of a significant interaction, we performed a conjunction analysis (Real AND Imagery) of the crucial contrast between CL and LL, confirming that all areas showing a coupling effect did so in both tasks (Supplementary Fig. 2 and Inline Supplementary Table S5). These areas were also significantly activated in the contrast between the bimanual CL and unimanual L conditions, in both Real and Imagery tasks (Supplementary Figs. 1b and d), further supporting the similarity of the brain activity in the Non-congruent conditions of both tasks.

Bimanual coupling within components of the medial wall motor areas

Based on anatomical, physiological and functional criteria, the SMA subdivides into a rostral SMA (the pre-SMA) and a caudal SMA (the SMA proper) (Matelli et al., 1991; Mayka et al., 2006; Picard and Strick, 1996). The border separating the SMA proper and the more anterior pre-SMA may, therefore, be the ventral anterior commissure plane. From a functional point of view, the general consensus appears to be that the pre-SMA participates in the selection and updating of movements, rather than in the initiation of the movement itself, whereas the SMA proper is more involved in the preparation of actual motor execution (Shima and Tanji, 2000; Picard and Strick, 2001). A similar functional distinction can be applied to the underlying CMA that has often been discussed together with the SMA and pre-SMA (e.g., Picard and Strick, 2001; Shackman et al., 2011). The present work classified the pre-SMA and the SMA proper according to Mayka et al. (2006). As shown in the Results (Tables 1 and 2), the ratio between SMA and pre-SMA is opposite for the Task and the Coupling factors (SMA/pre-SMA = 100/0%; SMA/pre-SMA = 36/64%, respectively).

Even if the critical role of the SMA in mediating bimanual asymmetric movements has been extensively described (e.g., Aramaki et al., 2006a; Debaere et al., 2004; Ehrsson et al., 2002; Immisch et al., 2001; Matsuda et al., 2009; Meyer-Lindenberg et al., 2002; Sadato et al., 1997; Wenderoth et al., 2004), the present results suggest a clear distinction between the functional role of SMA proper and pre-SMA in bimanual coupling. Consistent with the functional role of the SMA proper in the preparation of motor execution, activity of this area and of the underlying CMA (BA 31) was observed together with a right motor network as the main effect of Task (Fig. 5a), differentiating between the Real and Imagery tasks. For the SMA, the coordinates of peak activity appear very similar across previous studies (e.g. in Sadato et al., 1997: $x = 16$, $y = -20$ mm, $z = 64$ mm; in Wenderoth et al., 2004: $x = 12$, $y = -6$ mm, $z = 68$ mm; reported in MNI space). These coordinates are consistent with those found in the present study, although in our results the SMA coordinates are included in the CMA cluster with lower z values (see Table 1). Consistent with the functional role of the pre-SMA in abstract motor planning, this area (and the underlying pre-CMA) showed a Coupling effect (Fig. 5b), discriminating between Congruent (LL) and Non-congruent (CL) movements that was present in both Real and Imagery tasks as demonstrated by the conjunction result (Supplementary Fig. 2). Furthermore, the coupling specificity ($\text{CL} > \text{LL}$) of the pre-SMA/CMA with respect to the SMA/CMA was also confirmed by directly comparing the activity of these two areas in both Real ($p < 0.001$) and Imagery ($p = 0.007$) tasks.

Different interpretations have been placed on pre-SMA function that, according to Nachev et al. (2008), can be conceptually related to the complexity of their condition–action associations. Within this context, the conflict-monitoring hypothesis can be usefully applied in interpreting the present work. Based on this hypothesis, it has been suggested that the pre-SMA acts to resolve the response conflict between incompatible motor plans so that the desired action can be selected (e.g., Nachev et al., 2005). In the Non-congruent (CL) conditions, the monitoring of conflict between incompatible motor plans (Circles and Lines) can explain the activity of the pre-SMA in both Real and Imagery CL conditions. In accordance with this interpretation, a study on bimanual reaching (Diedrichsen et al., 2006) found that the pre-SMA and the pre-CMA showed increased activation not during bimanual actions per se, but only during asymmetric actions in a symbolic cuing condition (i.e., the activity was not observed when movement goals were spatially specified). This led the authors to propose that the role of these areas in bimanual motor control extends from their roles in monitoring goal-selection conflict. Apart from the left lateralization of this pre-SMA/CMA activity, which Diedrichsen et al. (2006) interpreted as occurring due to the symbolic nature of their task, the coordinates of peak activity ($x = -10$, $y = 22$ mm, $z = 46$ mm; reported in MNI space) are very similar to those found in the present study (see Table 2). Moreover, in bimanual situations when the conflict between incompatible motor

plans was absent (such as in the LL condition of the present study) activity of the pre-SMA was not found. Also consistent with our results, and considering the contrast between Real bimanual Congruent (LL) and unimanual L (see Supplementary Fig. 1a and Inline Supplementary Table S1), Toyokura et al. (2002) only found activity in the SMA proper and not in the pre-SMA when investigating the contrast between unimanual and bimanual thumb–finger oppositions in a mirror–symmetric fashion. However, Wenderoth et al. (2005b) reported the activity of the pre-SMA/CMA ($x = -4$, $y = 4$ mm, $z = 52$ mm; reported in MNI space) in the contrast between unimanual and bimanual movements, either when bimanual movements were Congruent (StarStar) or Non-congruent (LineStar). Importantly, this activity was higher for the LineStar than for the StarStar condition, indicating that such activity not only pertains to the bimanual modality per se, but is also modulated by the degree of spatial interference. Indeed, in our supplementary contrast between bimanual (CL or LL) and unimanual movements (L), greater pre-SMA/CMA activity was found in the contrast involving the Non-congruent (CL) condition, in both Real and Imagery tasks (Supplementary Fig. 1; Inline Supplementary Table S1–S4).

Other lines of research underline the role of the pre-SMA in motor inhibition processing. In fMRI studies, the role of the pre-SMA (and usually also the anterior cingulate) has been identified in go/no-go paradigms, with greater activity related to trials for which participants successfully cancel a response, compared to trials for which they do not (e.g., Amanzio et al., 2011; Sharp et al., 2010). Neurophysiologic studies (e.g., Swann et al., 2012) and TMS studies (e.g., Cai et al., 2012) show activation of the pre-SMA prior to and during stopping actions. Pertinent to the present work, the pre-SMA activity in the CL condition likely exerted an inhibitory function on the default coupling of homologous muscles, promoted by neural crosstalk (Cattaert et al., 1999), thus allowing the execution of Non-congruent movements (Sadato et al., 1997). An important role of motor inhibition processing has been described in motor imagery, in which the overt motor act has to be stopped (Kasess et al., 2008; Raffin et al., 2012). In our Imagery task, the pre-SMA activity can be explained by an increased recruitment of inhibitory processing in the Imagery Non-congruent condition, in which subjects performed right hand lines and simultaneously imagined performing left hand circles.

Another function typically ascribed to the pre-SMA, namely the motor learning of complex actions (e.g., Hikosaka et al., 1996; Nakamura et al., 1998), is also consistent with the present work. This fMRI study involved testing of naïve subjects; motor learning processing was very likely more involved for the Non-congruent (CL) conditions than for the Congruent (LL) conditions, which could be executed much more automatically. It is important to realize, therefore, that some of the observed activations related to bimanual coupling may represent only an intermediate stage when participants were initially confronted with an unfamiliar motor task. Learning allows participants to integrate movement patterns into one functional unit (Swinnen and Wenderoth, 2004) and it is likely that some of the observed brain activations would diminish (such as in pre-SMA) with further task repetition. Future experiments can be designed to investigate the relevance of motor learning in more detail, for example by comparing the pre-SMA activity during the Circles–Lines task in naïve and well-trained subjects (see also De Weerd et al., 2003).

In summary, these various interpretations of pre-SMA activity in the present study, and generally in the pre-SMA literature, reflect the fact that the pre-SMA has multiple functional subregions (Zhang et al., 2012) that can be selectively involved in different components of motor control.

Critical role of the posterior parietal cortex (PPC) in bimanual Non-congruent conditions

Like the medial wall motor areas, a functional distinction between regions subserving motor execution or motor intention and planning has been described for the parietal cortex (e.g., Gerardin et al., 2000). The activity of the primary (S1, involving BA 3, 2, 1) and secondary

(S2, involving BA 40 and 43) somatosensory areas in the anterior parietal lobe has been extensively associated with execution of hand movements, and this is interpreted as reflecting sensory feedback processes (e.g., Gerardin et al., 2000; Raffin et al., 2012; Sacco et al., 2009). In the present study, the activity of both S1 and S2 areas was mainly associated with the Real task, resulting from the actual execution of left hand movements (see Fig. 5a and Table 1). The S1 area also showed a Coupling effect, with greater activity in the CL condition than in the LL condition (see Fig. 5b and Table 2).

Beyond the comparatively straightforward interpretation of anterior parietal regions, the posterior parietal cortex (PPC) has been proposed to play a critical, multifaceted role in higher-level cognitive functions related to action (for a review, see Andersen and Buneo, 2002). Among these higher cognitive functions there is the formation of intentions or early plans for movement. Nonhuman primate research suggests that PPC contains a “map of intentions”, with different subregions dedicated to the planning of eye, reaching, and grasping movements (Andersen and Buneo, 2002), and that PPC activity is highly correlated with processes of motor planning (Quiñan Quiroga et al., 2006). Neuroimaging data on cognitive functions of human PPC provide information about involvement of this brain region in highly abstract motor programming (Culham and Kanwisher, 2001). Furthermore, electrical stimulation of the inferior parietal cortex during awake surgery (Desmurget et al., 2009) causes patients to intend to move and to report having moved, even in the absence of an actual motor response (i.e., the specific intention is not carried out).

In the present work, PPC activity was a main effect of the Coupling factor, irrespective of task, Real or Imagery (see Fig. 5b and Table 2). Bilateral PPC also showed consistent activation in the CL > LL contrast across Real and Imagery tasks, as demonstrated by the conjunction analysis (see Supplementary Fig. 2 and Inline Supplementary Table S5). Additionally, for bimanual versus unimanual contrasts in both tasks, PPC activity was found only when the Non-congruent CL condition was involved (i.e., CL > L; see Supplementary Figs. 1b and c, Inline Supplementary Tables S2 and S4). Taken together with the pre-SMA activity, the PPC activity (particularly in the IPL) supports the hypothesis that real and imagined Non-congruent movements activate common circuits related to intentional and predictive operation (Desmurget and Sirigu, 2009; Haggard, 2008), generating bimanual coupling. This finding is in keeping with behavioral results suggesting that directional interference primarily emerges at the efferent level of movement planning and organization (Swinnen et al., 2003). There is also fMRI evidence consistent with neuropsychological studies based on the behavior of brain-damaged patients (Garbarini et al., 2012; Garbarini et al., 2013) as well as of amputees with phantom limb phenomena (Franz and Ramachandran, 1998), which shows that the necessary component for bimanual coupling to occur is not the actual movement execution, but motor intention and programming.

Alternatively, the activity of the PPC (particularly the right SPL) can be explained by the “spatial” connotation of the tasks employed in the present work. The direct comparison between right and left SPL activity showed a greater involvement of the right SPL only in the Real task ($p = 0.035$). This standpoint is supported by research indicating that the parietal cortex may represent an important locus for integrating spatial aspects of limb movements into a common action. Wenderoth et al. (2004) investigated the neural correlates of bimanual spatial coupling, suggesting a central role of the right SPL in mediating spatial interference. These authors hypothesized that the right SPL is a candidate structure for where interference arises when directionally incompatible movements are performed. They discussed the possibility that interference emerges when computational resources in these parietal areas are insufficient to code two incompatible movement directions independently from each other (see also Wenderoth et al., 2005a, 2005b). This view is also supported by findings in split-brain patients showing that transection of the posterior corpus callosum, connecting the parietal cortices, abolishes directional interference during bimanual drawing

movements (Eliassen et al., 1999; Franz et al., 1996). Consistent with this interpretation, the study of Diedrichsen et al. (2006; see above) on bimanual congruent and Non-congruent reaching showed greater activation for Non-congruent movements in the SPL, making this region a likely neural site for the spatial interference that arises during execution of bimanual movements. The present work is consistent with this role for the SPL, showing increased activity during the Non-congruent movement whether the movement was executed or imagined. For the right SPL, the coordinates of peak activity are consistent across these studies (e.g. Wenderoth et al., 2004: $x = 30$, $y = -50$ mm, $z = 66$ mm; Wenderoth et al., 2005a: $x = 20$, $y = -56$ mm, $z = 66$ mm; Wenderoth et al., 2005b: $x = 30$, $y = -56$ mm, $z = 62$ mm; Diedrichsen et al., 2006: $x = 28$, $y = -70$ mm, $z = 60$ mm; reported in MNI space) and are also consistent with those found in the present study (Table 2). This suggests that the trigger for activating this brain region for the interference effect is not the afferent information coming from the somatosensory system, but the efferent information coming from the intentional and predictive operation implementing the Non-congruent motor program, irrespective of Real or Imagery task.

Left lateralization for the Imagery task

Previous neuroimaging data have also shown specific involvement of the PPC in motor imagery (Fleming et al., 2010; Gerardin et al., 2000; Hanakawa et al., 2008; Sacco et al., 2006) and also in bimanual motor imagery (Nair et al., 2003). Some studies have found bilateral involvement of the PPC (Fleming et al., 2010), while others have stressed the specific role of the left PPC (Gerardin et al., 2000). The evidence that the left hemisphere plays a dominant role in motor imagery stems from different lines of research. Left-brain-damaged patients are more impaired in motor imagery tasks than right-brain-damaged patients (Daprati et al., 2000), and only lesions of the left parietal lobe seem to produce motor imagery impairments of both hands (Sirigu et al., 1996). In addition, studies in healthy subjects involving various neurophysiological techniques have shown increased activity in left premotor, supplementary motor and parietal cortices, or enhanced excitability of the left Primary Motor Cortex during motor imagery (Bonda et al., 1995; Fadiga et al., 1999; Kuitz-Buschbeck et al., 2003; Stinear et al., 2006).

The present work is consistent with these lines of evidence, suggesting a left lateralization for the Imagery task and showing a specific role of the left IPL. The direct comparison between right and left IPL activity showed a greater involvement of the left IPL only in the Imagery task ($p = 0.045$). Before multiple comparisons correction, a greater activity was found for the Imagery task compared to the Real task in the left hemisphere, including the dorsolateral prefrontal cortex (DLPFC, BA 9), the PMCd (BA 6), the supramarginal gyrus (SMG, BA 40), and the bilateral posterior CRB. However, these activations showed only a trend toward statistical significance and did not survive multiple comparisons correction. A difference in lateralization, right for the Real and left for the Imagery task, was also found in the supplementary bimanual versus unimanual contrasts $CL > L$ and $LL > L$ (see Supplementary Fig. 1, Inline Supplementary Tables S1–S4 and Lateralization plots in Supplementary Figs. 9–16). As expected, the Real contrasts ($CL > L$; $LL > L$) showed a strongly right-lateralized motor network related to execution of the left hand movements. Conversely, the Imagery task showed bilateral activity of the medial wall motor areas in both the $CL > L$ and $LL > L$ contrasts and, only in the $CL > L$ contrast, activity in the bilateral anterior insula, the bilateral DLPFC, and in the left IPL, including the left SMG. Differences were also observed between the Real and Imagery tasks in cerebellar and frontal activity. See Supplementary discussion on CRB in SOM.

Limitations of the study

Although the sample size was justified by a power analysis based on previous literature (see SOM), the small sample size is the predominant limitation of the present study. This limitation is attenuated by the fact

that single-subject analysis confirmed the major results of group analysis, for both behavioral (Inline Supplementary Table S6) and imaging (Inline Supplementary Table S7) data.

Conclusion

The present experiment indicates that imagining and executing Non-congruent movements activate common circuits related to the intentional and predictive operation generating bimanual coupling, in which the right pre-SMA/CMA and bilateral PPC play a crucial role. In addition, the data also support a specific role of the right SPL in mediating spatial interference (Wenderoth et al., 2004) and of the left PPC in motor imagery (Gerardin et al., 2000). These findings are in line with previous studies on both healthy subjects (Swinnen et al., 2003) and neurological patients (Franz and Ramachandran, 1998; Garbarini et al., 2012; Garbarini et al., 2013) showing that directional interference primarily emerges at the efferent level of movement planning and organization. The work also motivates future studies using the Circles–Lines fMRI paradigm to investigate the neural correlates of the “illusion of movement”, described in pathological situations such as the phantom limb or anosognosia for hemiplegia, in which previous behavioral findings (Franz and Ramachandran, 1998; Garbarini et al., 2012) suggested the presence of bimanual coupling effects even in absence of actual movement execution.

Supplementary data to this article can be found online at <http://dx.doi.org/10.1016/j.neuroimage.2013.10.061>.

Acknowledgments

This study was funded by a Compagnia di San Paolo grant and a MIUR-PRIN grant (to A.B.). We are grateful to Luca Turella for his suggestions on the first draft of the paper. We are also indebted to the late Jon Driver for his helpful comments on the preliminary data of the study and to the anonymous reviewers who provided crucial suggestions regarding the fMRI data analysis.

References

- Amanzio, M., Torta, D.M., Sacco, K., Cauda, F., D'Agata, F., Duca, S., Leotta, D., Palermo, S., Geminiani, G.C., 2011. Unawareness of deficits in Alzheimer's disease: role of the cingulate cortex. *Brain* 134, 1061–1076.
- Andersen, R.A., Buneo, C.A., 2002. Intentional maps in posterior parietal cortex. *Annu. Rev. Neurosci.* 25, 189–220.
- Aramaki, Y., Honda, M., Sadato, N., 2006a. Suppression of the non-dominant motor cortex during bimanual symmetric finger movement: a functional magnetic resonance imaging study. *Neuroscience* 141, 2147–2153.
- Aramaki, Y., Honda, M., Okada, T., Sadato, N., 2006b. Neural correlates of the spontaneous phase transition during bimanual coordination. *Cereb. Cortex* 16, 1338–1348.
- Banerjee, A., Tognoli, E., Kelso, J.A., Jirsa, V.K., 2012. Spatiotemporal re-organization of large-scale neural assemblies underlies bimanual coordination. *Neuroimage* 62, 1582–1592.
- Bonda, E., Petrides, M., Frey, S., Evans, A., 1995. Neural correlates of mental transformations of the body-in-space. *Proc. Natl. Acad. Sci.* 92, 11180–11184.
- Boynton, G.M., Engel, S.A., Glover, G.H., Heeger, D.J., 1996. Linear systems analysis of functional magnetic resonance imaging in human V1. *J. Neurosci.* 16, 4207–4221.
- Cai, W., George, J.S., Verbruggen, F., Chambers, C.D., Aron, A.R., 2012. The role of the right presupplementary motor area in stopping action: two studies with event-related transcranial magnetic stimulation. *J. Neurophysiol.* 108, 380–389.
- Cattaert, D., Semjen, A., Summers, J.J., 1999. Simulating a neural cross talk model for between-hand interference during bimanual circle-drawing. *Biol. Cybern.* 81, 343–358.
- Culham, J.C., Kanwisher, N.G., 2001. Neuroimaging of cognitive functions in human parietal cortex. *Curr. Opin. Neurobiol.* 11, 157–163.
- Daprati, E., Sirigu, A., Pradat-Diehl, P., Frank, N., Jeannerod, M., 2000. Recognition of self-produced movements in a case of severe neglect. *Neurocase* 6, 477–486.
- De Weerd, P., Reinke, K., Ryan, L., Mclsaac, T., Perschler, P., Schnyer, D., Trouard, T., Gmitro, A., 2003. Cortical mechanisms for acquisition and performance of bimanual motor sequences. *Neuroimage* 19, 1405–1416.
- Debaere, F., Wenderoth, N., Sunaert, S., Hecke, P.V., Swinnen, S.P., 2004. Cerebellar and premotor function in bimanual coordination: parametric neural responses to spatio-temporal complexity and cycling frequency. *Neuroimage* 21, 1416–1427.
- Desmurget, M., Sirigu, A., 2009. A parietal-premotor network for movement intention and motor awareness. *Trends Cogn. Sci.* 13, 411–419.
- Desmurget, M., Reilly, K.T., Richard, N., Szathmari, A., Mottolese, C., Sirigu, A., 2009. Movement intention after parietal cortex stimulation in humans. *Science* 324, 811–813.

- Diedrichsen, J., Grafton, S., Albert, N., Hazeltine, E., Ivry, R.B., 2006. Goal-selection and movement-related conflict during bimanual reaching movements. *Cereb. Cortex* 16, 1729–1738.
- Dounskaia, N., Nogueira, K.G., Swinnen, S.P., Drummond, E., 2010. Limitations on coupling of bimanual movements caused by arm dominance: when the muscle homology principle fails. *J. Neurophysiol.* 103, 2027–2038.
- Ehrsson, H.H., Kuhtz-Buschbeck, J.P., Forssberg, H., 2002. Brain regions controlling nonsynergistic versus synergistic movement of the digits: a functional magnetic resonance imaging study. *J. Neurosci.* 22, 5074–5080.
- Ehrsson, H.H., Geyer, S., Naito, E., 2003. Imagery of voluntary movement of fingers, toes, and tongue activates corresponding body-part-specific motor representations. *J. Neurophysiol.* 90, 3304–3316.
- Eliassen, J.C., Baynes, K., Gazzaniga, M.S., 1999. Direction information coordinated via the posterior third of the corpus callosum during bimanual movements. *Exp. Brain Res.* 128, 573–577.
- Fadiga, L., Buccino, G., Craighero, L., Fogassi, L., Gallese, V., Pavesi, G., 1999. Corticospinal excitability is specifically modulated by motor imagery: a magnetic stimulation study. *Neuropsychologia* 37, 147–158.
- Fleming, M.K., Stinear, C.M., Byblow, W.D., 2010. Bilateral parietal cortex function during motor imagery. *Exp. Brain Res.* 201, 499–508.
- Forman, S.D., Cohen, J.D., Fitzgerald, M., Eddy, W.F., Mintun, M.A., Noll, D.C., 1995. Improved assessment of significant activation in functional magnetic resonance imaging (fMRI): use of a cluster-size threshold. *Magn. Reson. Med.* 33 (5), 636–647.
- Frak, V., Paulignan, Y., Jeannerod, M., 2001. Orientation of the opposition axis in mentally simulated grasping. *Exp. Brain Res.* 136, 120–127.
- Franz, E.A., 2003. Bimanual action representation: a window on human evolution. In: Johnson-Frey, S.H. (Ed.), *Taking Action: Cognitive Neuroscience Perspectives on Intentional Acts*. The MIT Press, Cambridge, pp. 259–288.
- Franz, E.A., Ramachandran, V.S., 1998. Bimanual coupling in amputees with phantom limbs. *Nat. Neurosci.* 1, 443–444.
- Franz, E.A., Zelaznik, H.N., McCabe, G., 1991. Spatial topological constraints in a bimanual task. *Acta Psychol.* 77, 137–151.
- Franz, E.A., Eliassen, J.C., Ivry, R.B., Gazzaniga, M.S., 1996. Dissociation of spatial and temporal coupling in the bimanual movements of callosotomy patients. *Psychol. Sci.* 7, 306–310.
- Garbarini, F., Rabuffetti, M., Piedimonte, A., Pia, L., Ferrarin, M., Frassinetti, F., Gindri, P., Cantagallo, A., Driver, J., Berti, A., 2012. “Moving” a paralyzed hand: bimanual coupling effect in anosognosic patients. *Brain* 135, 1486–1497.
- Garbarini, F., Pia, L., Piedimonte, A., Rabuffetti, M., Gindri, P., Berti, A., 2013. Embodiment of an alien hand interferes with intact-hand movements. *Curr. Biol.* 23, 57–58.
- Gerardin, E., Sirigu, A., Lehéry, S., Poline, J.B., Gaymard, B., Marsault, C., Agid, Y., Le Bihan, D., 2000. Partially overlapping neural networks for real and imagined hand movements. *Cereb. Cortex* 10, 1093–1104.
- Goebel, R., Esposito, F., Formisano, E., 2006. Analysis of functional image analysis contest (FIAC) data with Brain Voyager QX: from single-subject to cortically aligned group general linear model analysis and self-organizing group independent component analysis. *Hum. Brain Mapp.* 27, 392–401.
- Grefkes, C., Eickhoff, S.B., Nowak, D.A., Dafotakis, M., Fink, G.R., 2008. Dynamic intra and interhemispheric interactions during unilateral and bilateral hand movements assessed with fMRI and DCM. *Neuroimage* 41, 1382–1394.
- Gregg, M., Hall, C., Butler, A., 2010. The MIQ-RS: a suitable option for examining movement imagery ability. *Evid.-Based Complement. Altern. Med.* 7, 249–257.
- Haggard, P., 2008. Human volition: towards a neuroscience of will. *Nat. Rev. Neurosci.* 9, 934–946.
- Hanakawa, T., Dimyan, M.A., Hallett, M., 2008. Motor planning, imagery, and execution in the distributed motor network: a time-course study with functional MRI. *Cereb. Cortex* 18, 2775–2788.
- Henson, R., 2005. What can functional neuroimaging tell the experimental psychologist? *Q. J. Exp. Psychol.* A 58 (2), 193–233.
- Hikosaka, O., Sakai, K., Miyauchi, S., Takino, R., Sasaki, Y., Pütz, B., 1996. Activation of human presupplementary motor area in learning of sequential procedures: a functional MRI study. *J. Neurophysiol.* 76, 617–621.
- Immisch, I., Waldvogel, D., van Gelderen, P., Hallett, M., 2001. The role of the medial wall and its anatomical variations for bimanual antiphase and in-phase movements. *Neuroimage* 14, 674–684.
- Jeannerod, M., Frak, V., 1999. Mental imaging of motor activity in humans. *Curr. Opin. Neurobiol.* 9, 735–739.
- Kasess, C.H., Windischberger, C., Cunnington, R., Lanzenberger, R., Pezawas, L., Moser, E., 2008. The suppressive influence of SMA on M1 in motor imagery revealed by fMRI and dynamic causal modeling. *Neuroimage* 40, 828–837.
- Kelso, J.A., 1984. Phase transitions and critical behavior in human bimanual coordination. *Am. J. Physiol.* 246, R1000–R1004.
- Kelso, J.A., Southard, D.L., Goodman, D., 1979. On the coordination of two-handed movements. *J. Exp. Psychol. Hum. Percept. Perform.* 5, 229–238.
- Klapp, S.T., 1979. Doing two things at once: the role of temporal compatibility. *Mem. Cognit.* 1, 375–381.
- Koeneke, S., Lutz, K., Wüstenberg, T., Jänke, L., 2004. Bimanual versus unimanual coordination: what makes the difference? *Neuroimage* 22, 1336–1350.
- Kuhtz-Buschbeck, J.P., Mahnkopf, C., Holzknecht, C., Siebner, H., Ulmer, S., Jansen, O., 2003. Effector-independent representations of simple and complex imagined finger movements: a combined fMRI and TMS study. *Eur. J. Neurosci.* 18, 3375–3387.
- Macaluso, E., Cherubini, A., Sabatini, U., 2007. Bimanual passive movement: functional activation and inter-regional coupling. *Front. Integr. Neurosci.* 1, 1–5.
- Maki, Y., Wong, K.F., Sugiura, M., Ozaki, T., Sadato, N., 2008. Asymmetric control mechanisms of bimanual coordination: an application of directed connectivity analysis to kinematic and functional MRI data. *Neuroimage* 42, 1295–1304.
- Matelli, M., Luppino, G., Rizzolatti, G., 1991. Architecture of superior and mesial area 6 and the adjacent cingulate cortex in the macaque monkey. *J. Comp. Neurol.* 311, 445–462.
- Matsuda, T., Watanabe, S., Kuruma, H., Murakami, Y., Watanabe, R., Senou, A., 2009. A comparison of three bimanual coordinations: an fMRI study. *J. Phys. Ther. Sci.* 25, 85–92.
- Mayka, M.A., Corcos, D.M., Leurgans, S.E., Vaillancourt, D.E., 2006. Three-dimensional locations and boundaries of motor and premotor cortex as defined by functional brain imaging: a meta-analysis. *Neuroimage* 31, 1453–1474.
- Meyer-Lindenberg, A., Ziemann, U., Hajak, G., Cohen, L., Berman, K.F., 2002. Transitions between dynamical states of differing stability in the human brain. *Proc. Natl. Acad. Sci. U. S. A.* 99, 10948–10953.
- Mulder, T., Hochstenbach, J.B., van Heuvelen, M.J., den Otter, A.R., 2007. Motor imagery: the relation between age and imagery capacity. *Hum. Mov. Sci.* 26, 203–211.
- Nachev, P., Rees, G., Parton, A., Kennard, C., Husain, M., 2005. Volition and conflict in human medial frontal cortex. *Curr. Biol.* 15, 122–128.
- Nachev, P., Kennard, C., Husain, M., 2008. Functional role of the supplementary and pre-supplementary motor areas. *Nat. Rev. Neurosci.* 9, 856–869.
- Nair, D.G., Purcott, K.L., Fuchs, A., Steinberg, F., Kelso, J.A., 2003. Cortical and cerebellar activity of the human brain during imagined and executed unimanual and bimanual action sequences: a functional MRI study. *Brain Res. Cogn. Brain Res.* 15, 250–260.
- Nakamura, K., Sakai, K., Hikosaka, O., 1998. Neuronal activity in medial frontal cortex during learning of sequential procedures. *J. Neurophysiol.* 80, 2671–2687.
- Nichols, T., Brett, M., Andersson, J., Wager, T., Poline, J.-B., 2005. Valid conjunction inference with the minimum statistic. *Neuroimage* 25, 653–660.
- Oldfield, R.C., 1971. The assessment and analysis of handedness: the Edinburgh inventory. *Neuropsychologia* 9, 97–113.
- Parsons, L.M., 2001. Integrating cognitive psychology, neurology and neuroimaging. *Acta Psychol. (Amst)* 107, 155–181.
- Personnier, P., Paizis, C., Ballay, Y., Papaxanthis, C., 2008. Mentally represented motor actions in normal aging II. The influence of the cortico-inertial context on the duration of overt and covert arm movements. *Behav. Brain Res.* 25 (186), 273–283.
- Peters, M., 1977. Simultaneous performance of two motor activities: the factor of timing. *Neuropsychologia* 15, 461–465.
- Pia, L., Spinazzola, L., Rabuffetti, M., Ferrarin, M., Garbarini, F., Piedimonte, A., Driver, J., Berti, A., 2013. Temporal coupling due to illusory movements in bimanual actions: evidence from anosognosia for hemiplegia. *Cortex* 49, 1694–1703.
- Picard, N., Strick, P.L., 2001. Imaging the premotor areas. *Curr Opin Neurobiol.* 11, 663–672.
- Picard, N., Strick, P.L., 1996. Motor areas of the medial wall: a review of their location and functional activation. *Cereb. Cortex* 6, 342–353.
- Porro, C.A., Cettolo, V., Francescato, M.P., Baraldi, P., 2000. Ipsilateral involvement of primary motor cortex during motor imagery. *Eur. J. Neurosci.* 12, 3059–3063.
- Quian Quiroga, R., Snyder, L.H., Batista, A.P., Cui, H., Andersen, R.A., 2006. Movement intention is better predicted than attention in the posterior parietal cortex. *J. Neurosci.* 26, 3615–3620.
- Raffin, E., Mattout, J., Reilly, K.T., Giroux, P., 2012. Disentangling motor execution from motor imagery with the phantom limb. *Brain* 135, 582–595.
- Sacco, K., Cauda, F., Cerliani, L., Mate, D., Duca, S., Geminiani, G.C., 2006. Motor imagery of walking following training in locomotor attention. The effect of “the tango lesson”. *Neuroimage* 32, 1441–1449.
- Sacco, K., Cauda, F., D’Agata, F., Mate, D., Duca, S., Geminiani, G., 2009. Reorganization and enhanced functional connectivity of motor areas in repetitive ankle movements after training in locomotor attention. *Brain Res.* 1297, 124–134.
- Sadato, N., Yonekura, Y., Waki, A., Yamada, H., Ishii, Y., 1997. Role of the supplementary motor area and the right premotor cortex in the coordination of bimanual finger movements. *J. Neurosci.* 17, 9667–9674.
- Saimpont, A., Pozzo, T., Papaxanthis, C., 2009. Aging affects the mental rotation of left and right hands. *PLoS One* 4, e6714.
- Schmahmann, J.D., Doyon, J., McDonald, D., Holmes, C., Lavoie, K., Hurwitz, A.S., Kabani, N., Toga, A., Evans, A., Petrides, M., 1999. Three-dimensional MRI atlas of the human cerebellum in proportional stereotaxic space. *Neuroimage* 10, 233–260.
- Shackman, A.J., Salomons, T.V., Slagter, H., Fox, A.S., Winter, J.J., Davidson, R.J., 2011. The integration of negative affect, pain and cognitive control in the cingulate cortex. *Nat. Rev. Neurosci.* 12, 154–167.
- Sharp, D.J., Bonnello, V., De Boissezon, X., Beckmann, C.F., James, S.G., Patel, M.C., Mehta, M.A., 2010. Distinct frontal systems for response inhibition, attentional capture, and error processing. *Proc. Natl. Acad. Sci. U. S. A.* 107, 6106–6111.
- Shima, K., Tanji, J., 2000. Neuronal activity in the supplementary and presupplementary motor areas for temporal organization of multiple movements. *J. Neurophysiol.* 84, 2148–2160.
- Sirigu, A., Duhamel, J.R., Cohen, L., Pillon, B., Dubois, B., Agid, Y., 1996. The mental representation of hand movements after parietal cortex damage. *Science* 273, 1564–1568.
- Skoura, X., Personnier, P., Vinter, A., Pozzo, T., Papaxanthis, C., 2008. Decline in motor prediction in elderly subjects: right versus left arm differences in mentally simulated motor actions. *Cortex* 44, 1271–1278.
- Stinear, C.M., Fleming, M.K., Byblow, W.D., 2006. Lateralization of unimanual and bimanual motor imagery. *Brain Res.* 1095, 139–147.
- Swann, N.C., Cai, W., Pieters, T., Claffey, M.P., George, J.S., Connors, C., DiSano, M., Aron, A.R., Tandon, N., 2012. Roles for the presupplementary motor area and the right inferior frontal gyrus in stopping action: electrophysiological responses and functional and structural connectivity. *Neuroimage* 59, 2860–2870.

- Swinnen, S., 2002. Intermanual coordination: from behavioural principles to neural-network interactions. *Nat. Rev. Neurosci.* 3 (5), 348–359.
- Swinnen, S.P., Wenderoth, N., 2004. Two hands, one brain: cognitive neuroscience of bimanual skill. *Trends Cogn. Sci.* 8, 18–25.
- Swinnen, S.P., Jardin, K., Meulenbroek, R., Dounskaia, N., Hofkens-van den Brandt, M., 1997. Egocentric and allocentric constraints in the expression of patterns of interlimb coordination. *J. Cogn. Neurosci.* 9, 348–377.
- Swinnen, S., Dounskaia, N., Levin, O., Duysens, J., 2001. Constraints during bimanual coordination: the role of direction in relation to amplitude and force requirements. *Behav. Brain Res.* 123 (2), 201–218.
- Swinnen, S., Dounskaia, N., Duysens, J., 2002. Patterns of bimanual interference reveal movement encoding within a radial egocentric reference frame. *J. Cogn. Neurosci.* 14 (3), 463–471.
- Swinnen, S.P., Puttemans, V., Vangheluwe, S., Wenderoth, N., Levin, O., Dounskaia, N., 2003. Directional interference during bimanual coordination: is interlimb coupling mediated by afferent or efferent processes. *Behav. Brain Res.* 139, 177–195.
- Talairach, J., Tournoux, L., 1988. *Co-planar Stereotaxic Atlas of the Human Brain: 3-dimensional Proportional System – An Approach to Cerebral Imaging*. Thieme, New York.
- Tam, F., Churchill, N.W., Strother, S.C., Graham, S.J., 2011. A new tablet for writing and drawing during functional MRI. *Hum. Brain Mapp.* 32, 240–248.
- Toyokura, M., Muro, I., Komiya, T., Obara, M., 2002. Activation of pre-supplementary motor area (SMA) and SMA proper during unimanual and bimanual complex sequences: an analysis using functional magnetic resonance imaging. *J. Neuroimaging* 12 (1), 72–78.
- Walsh, R.R., Small, S.L., Chen, E.E., Solodkin, A., 2008. Network activation during bimanual movements in humans. *Neuroimage* 3, 540–553.
- Wenderoth, N., Debaere, F., Sunaert, S., Hecke, P., Swinnen, S.P., 2004. Parieto-premotor areas mediate directional interference during bimanual movements. *Cereb. Cortex* 14, 1153–1163.
- Wenderoth, N., Debaere, F., Sunaert, S., Swinnen, S., 2005a. Spatial interference during bimanual coordination: differential brain networks associated with control of movement amplitude and direction. *Hum. Brain Mapp.* 26 (4), 286–300.
- Wenderoth, N., Debaere, F., Sunaert, S., Swinnen, S., 2005b. The role of anterior cingulate cortex and precuneus in the coordination of motor behaviour. *Eur. J. Neurosci.* 22 (1), 235–246.
- Zhang, S., Ide, J.S., Li, C.S., 2012. Resting-state functional connectivity of the medial superior frontal cortex. *Cereb. Cortex* 22, 99–111.